Supplementary Information

Climate driven ground-level ozone extreme in the fall over the Southeast United States

Yuzhong Zhang[a], Yuhang Wang[a]

[a]School of Earth and Atmospheric Sciences, Georgia Institute of Technology, Atlanta, Georgia 30332, USA

Corresponding author: Yuhang Wang

School of Earth and Atmospheric Sciences, Georgia Institute of Technology, Atlanta, Georgia 30332, USA,

Phone: (480) 329-5831,

Email ywang@eas.gatech.edu

SI Text

Impact of stratospheric intrusion on surface ozone. We find that stratospheric intrusion is unlikely to be a major factor for surface ozone enhancements during Oct. 2010 episodes. The arguments are as follows.

First, stratospheric intrusion is often accompanied by a cut-off low pressure system at 500 hPa (1). However, such patterns do not coincide with the three surface-ozone episodes during the month, October 7–12, 16–18, and 21–24. Moreover, the cut-off low system favoring the stratospheric intrusion often ventilates ozone and its precursors out of the boundary layer and therefore is unfavorable to the ozone built-up at the surface (2). For example, on Oct. 4, 2010, when eastern US is under the influence of the cut-off low system at 500 hPa, the regional mean $[O_3]_{MDA8}$ over the SE is only 35 ppbv (Fig. 2A and Fig. S15a).

Second, no direct observational evidence has shown that stratospheric intrusion can impact surface ozone over the SE. In most cases, the intrusion is unable to penetrate the entire troposphere (2, 3). Moreover, stratospheric intrusion is usually found the weakest in the fall season (1). Our calculation using the REAM model also shows that the enhancement by stratospheric ozone is less than 1 ppbv below 600 hPa during the stratospheric intrusion event on Oct. 4, 2010 (Fig. S15b).

Explained Variance Decomposition (EVD) method. We use the explained variance decomposition (EVD) method to compute the attributions of correlated meteorological variables to the explained variance of ground-level ozone. Note that unlike in other sections, the variables used in this section are normalized for simplicity in mathematical derivations.

Given normalized variables, $[O_3]_{MDA8}$, T_{max}, and VPD, let EV be the coefficient of determination (R^2) for the bivariate model $[O_3]_{MDA8} \sim T_{max}$ + VPD. EV represents the fraction of total variance in $[O_3]_{MDA8}$ that can be explained by T_{max} and VPD. The EVD method described here decomposes $EV_{T\text{-}VPD}$ into three parts: a) variance solely explained by T_{max}, denoted as EV_T; b) variance solely explained by VPD, denoted as EV_{VPD}; and c) variance explained by the correlation between T_{max} and VPD, denoted as $EV_{T\text{-}VPD}$.

$$EV = EV_T + EV_{VPD} + EV_{T\text{-}VPD} \quad [1]$$

To calculate EV_T, EV_{VPD}, and $EV_{T\text{-}VPD}$, we first do the following transformation,

$$z_1 = T_{max} \quad [2]$$

$$z_2 = [-\frac{r}{\sqrt{1+r^2}}, \frac{1}{\sqrt{1+r^2}}][\begin{matrix} T_{max} \\ VPD \end{matrix}] \quad [3]$$

where r is the Pearson correlation coefficient between T_{max} and VPD. Note that z_1 and z_2 are orthogonal. A bivariate linear regression ($[O_3]_{MDA8} \sim z_1+z_2$) leads to:

$$[O_3]_{MDA8} = a \cdot z_1 + b \cdot z_2 + \varepsilon \quad [4]$$

where a and b are coefficients for z_1 and z_2, respectively, and ε is the error term. Since z_1 and z_2 contain the same amount of information as T_{max} and VPD do, R^2 for this model is also EV. Furthermore, since z_1 and z_2 are orthogonal, EV can be decomposed into two parts:

$$EV = a^2 \sum_i z_{1,i}^2 + b^2 \sum_i z_{2,i}^2 \quad [5]$$

where the second term is attributable to only VPD and the first term is attributable to both T_{max} and the correlation between T_{max} and VPD. Therefore, we have

$$EV_T + EV_{T-VPD} = a^2 \sum_i z_{1,i}^2 \quad [6]$$

$$EV_{VPD} = b^2 \sum_i z_{2,i}^2 \quad [7]$$

Similarly to Eqs. [2-4], we can also do the following transformation and regression:

$$z_3 = VPD \quad [8]$$

$$z_4 = [-\frac{r}{\sqrt{1+r^2}}, \frac{1}{\sqrt{1+r^2}}][\frac{\mathrm{VPD}}{T_{\max}}] \quad [9]$$

$$[O_3]_{MDA8} = c \cdot z_3 + d \cdot z_4 + \varepsilon \quad [10]$$

Using Eqs. [8-9], we have another decomposition of EV,

$$\mathrm{EV} = c^2 \sum_i z_{3,i}^2 + d^2 \sum_i z_{4,i}^2 \quad [11]$$

where the second term is attributable to only T_{max} and the first term is attributable to both VDP and the correlation between T_{max} and VPD.

$$\mathrm{EV_{VPD}} + \mathrm{EV_{T-VPD}} = c^2 \sum_i z_{3,i}^2 \quad [12]$$

$$\mathrm{EV_T} = d^2 \sum_i z_{4,i}^2 \quad [13]$$

Note Eqs. [6], [7], [12], [13] are not independent. Therefore, combining any three from these four equations, we can solve for EV_T , EV_{VPD}, and $EV_{T\text{-}VPD}$.

SI References

1 Singh HB, Viezee W, Johnson WB, & Ludwig FL (1980) The Impact of Stratospheric Ozone on Tropospheric Air Quality. *Journal of the Air Pollution Control Association* 30(9):1009-1017.

2 Ott LE, et al. (2016) Frequency and impact of summertime stratospheric intrusions over Maryland during DISCOVER-AQ (2011): New evidence from NASA's GEOS-5 simulations. *Journal of Geophysical Research: Atmospheres* 121(7):3687-3706.

3 Viezee W, Johnson WB, & Singh HB (1983) Stratospheric ozone in the lower troposphere—II. Assessment of downward flux and ground-level impact. *Atmospheric Environment (1967)* 17(10):1979-1993.

4 U.S. EPA (2015) National Emissions Inventory (NEI) Air Pollutant Emissions Trends Data, Available from https://www.epa.gov/air-emissions-inventories/air-pollutant-emissions-trends-data (Accessed 3 August 2016).

5 Potosnak MJ, et al. (2014) Observed and modeled ecosystem isoprene fluxes from an oak-dominated temperate forest and the influence of drought stress. *Atmospheric Environment* 84(0):314-322.

6 Seco R, et al. (2015) Ecosystem-scale volatile organic compound fluxes during an extreme drought in a broadleaf temperate forest of the Missouri Ozarks (central USA). *Global Change Biology* 21(10):3657-3674.

7 Pegoraro E, et al. (2005) The interacting effects of elevated atmospheric CO_2 concentration, drought and leaf-to-air vapour pressure deficit on ecosystem isoprene fluxes. *Oecologia* 146(1):120-129.

SI Figures

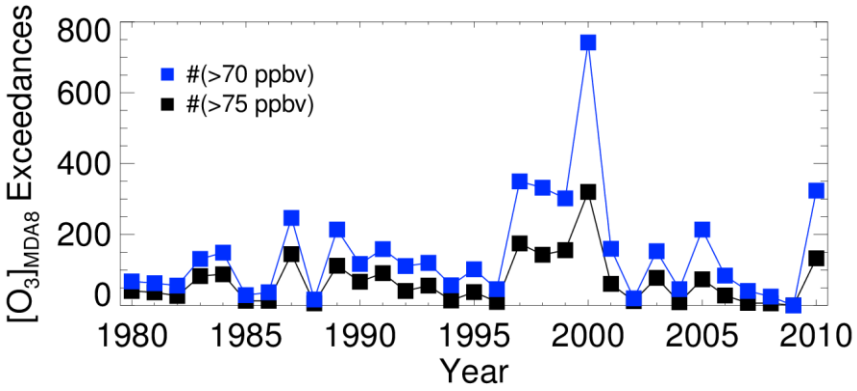

105

Figure S1. Occurrences of $[O_3]_{MDA8}$ at the EPA observation sites exceeding 70 ppbv (blue) and 75 ppbv (black) over the SE in October from 1980 to 2010.

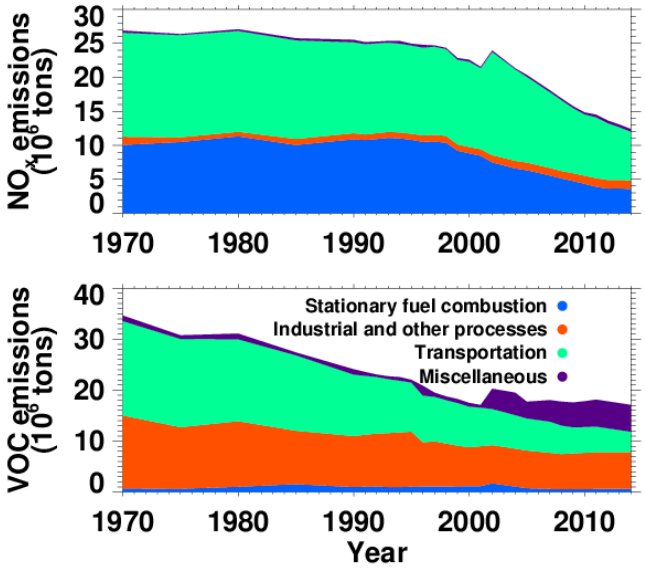

Figure S2. Emissions of NO_x and VOC from different sectors in the U.S. from 1970 to 2014. Adapted from U.S. EPA (4).

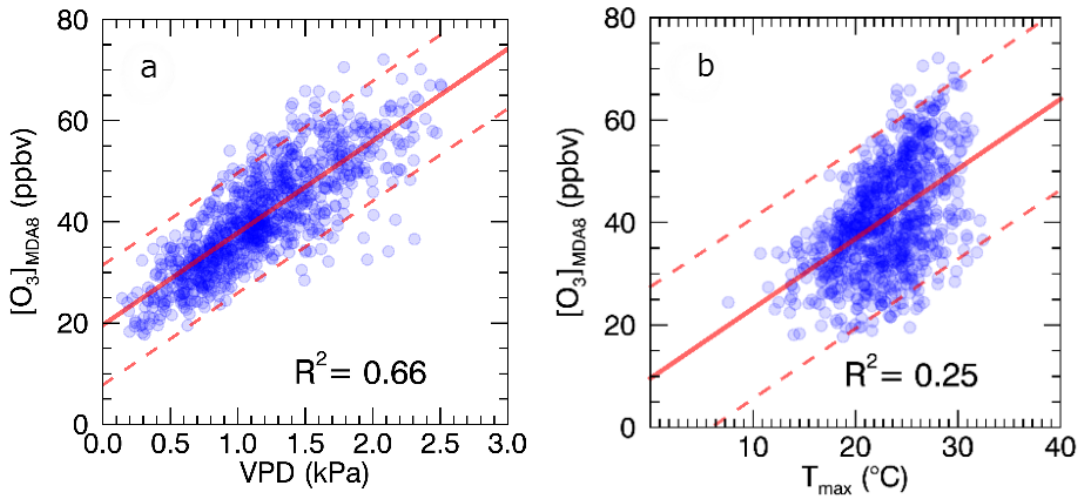

Figure S3. Relationship between daily $[O_3]_{MDA8}$ and daily meteorological variables (a, daytime VPD and b, T_{max}) over the SE in October from 1980 to 2010. Red solid lines in **a** and **b** are linear fits and red dash lines the 95th percentile confidence intervals.

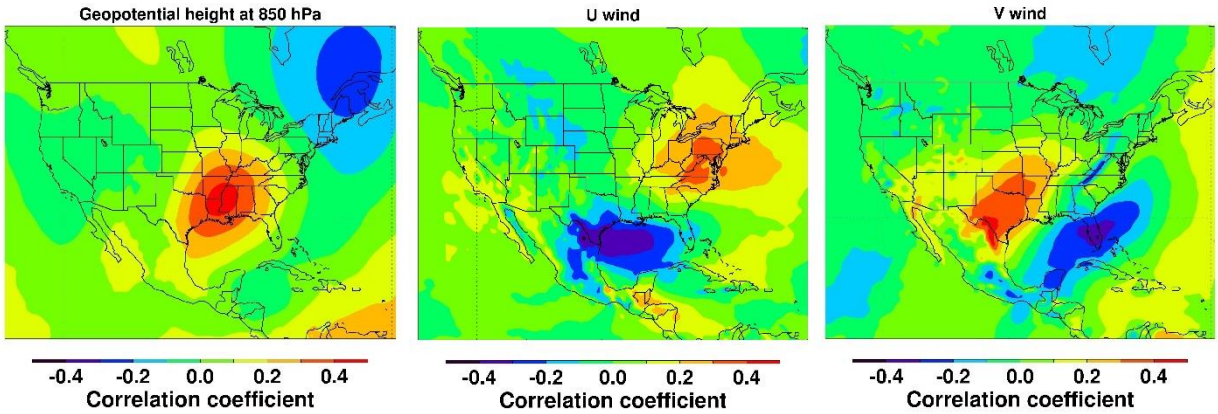

Figure S4. Correlations of 850 hPa geopotential height, surface u wind, and surface v wind with daytime VPD over the SE in October. Daily CFSR reanalysis data from 1980 to 2010 are used. The patterns are consistent with the presence of a high pressure system over the SE.

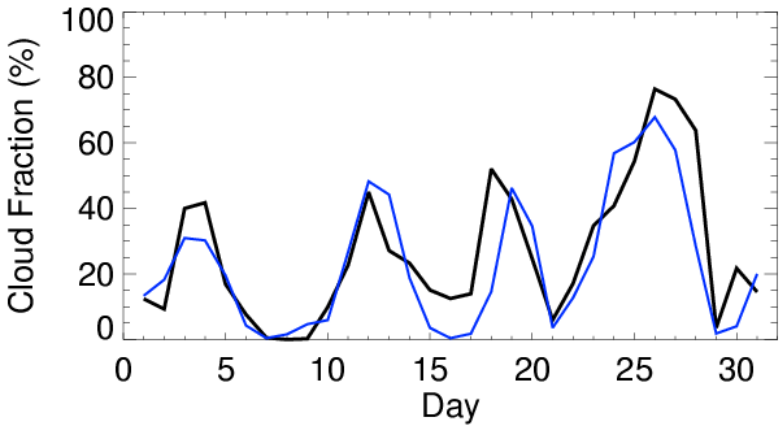

125 **Figure S5. Reanalyzed and WRF simulated cloud fraction over the SE in October 2010.** The black line is the CFSR reanalysis data. The blue solid line is the WRF simulated cloud fraction.

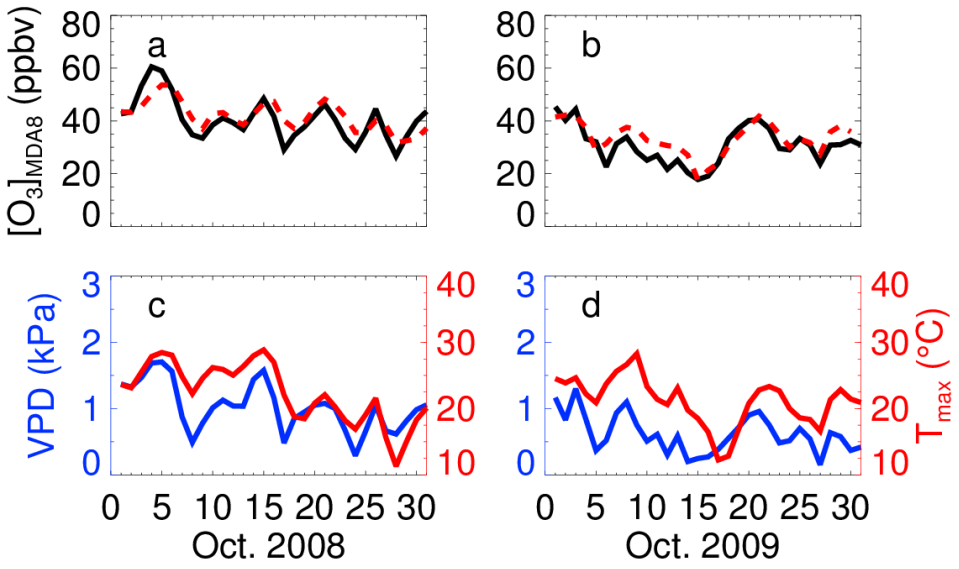

Figure S6. Simulated $[O_3]_{MDA8}$ in a normal-ozone month (October 2008) and a low-ozone month (October 2009) over the SE. a and b, Black solid lines are observations and red dashed lines are the base model simulation results. **c and d**, Blue lines are for daytime VPD and red lines for T_{max}. Meteorological data from CSFR reanalysis are used.

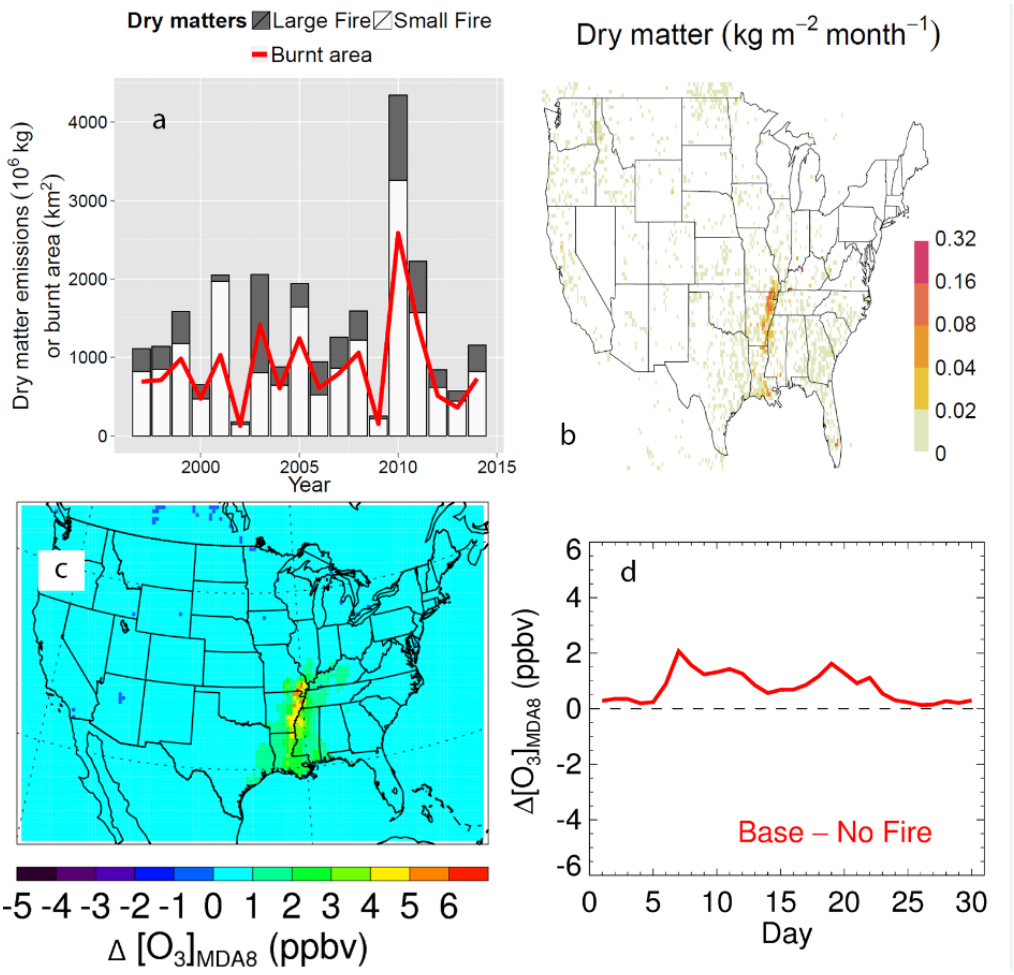

135

Figure S7. a, GFED4s burnt dry matters (bar) and burnt area (line) over the SE in October. Burnt dry matters from large and small fires are denoted with black and white bars, respectively. **b**, Spatial distribution of burnt dry matters from GFED4s in Oct. 2010. Spatial (**c**) and temporal (**d**) impacts of fire emissions on surface ozone ($[O_3]_{MDA8}$) over the SE in Oct. 2010.

140

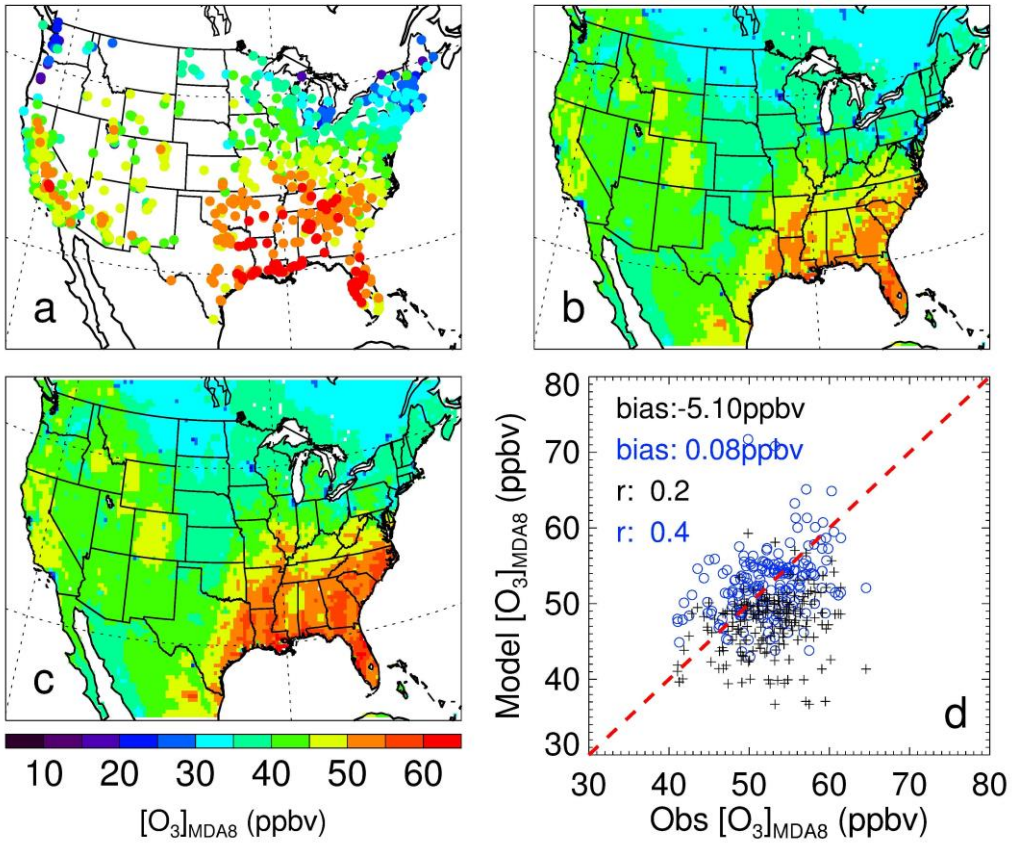

Figure S8. Doubled isoprene emissions improve agreement between observations and simulation. In comparison with observations (**a**), the base simulation (**b**) significantly underestimates the monthly mean $[O_3]_{MDA8}$ in the SE, whereas a simulation with doubled isoprene emissions (**c**) is able to reproduce the enhancement of $[O_3]_{MDA8}$ over the region. **d,** The simulation with doubled isoprene emissions (blue circles) is spatially in better agreement with observations than the base simulation (black cross). Each symbol represents the monthly average of $[O_3]_{MDA8}$ at a monitoring site. The red line is the 1:1 line. Biases and correlation coefficients (*r*) are shown.

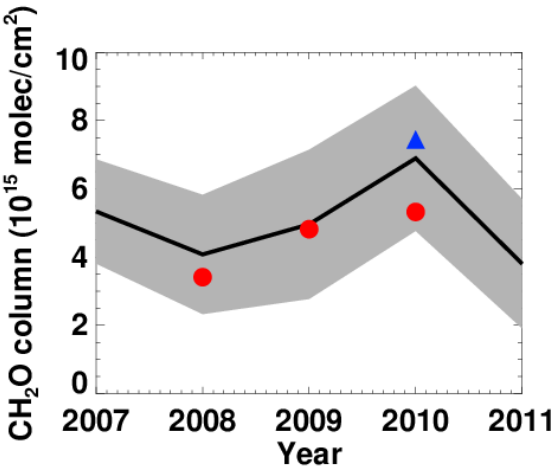

Figure S9. GOME-2 observed monthly mean CH_2O column densities (black) over the SE in October from 2007 to 2011 show a peak in 2010, implying large biogenic emissions. The simulated CH_2O column density with the standard MEGAN algorithm (red dots) is in agreement with GOME-2 in 2008 and 2009, but is biased low in 2010. Doubling biogenic emissions (blue triangle) in 2010 corrects the bias. The gray area shows the 1-σ spatial standard deviation over the region.

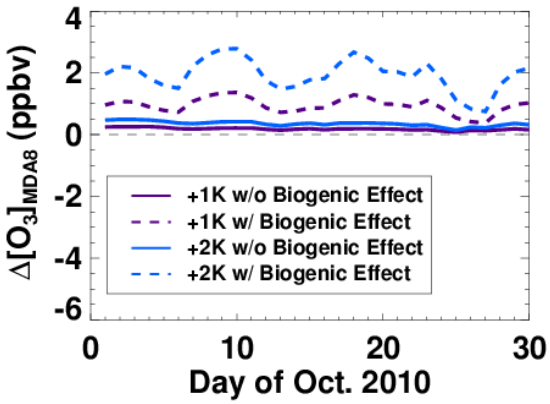

Figure S10. Response of surface ozone ($[O_3]_{MDA8}$) to perturbation of temperature with or without the effect of temperature on biogenic emissions shows that the uncertainties in these factors are inadequate to explain the underestimation of $[O_3]_{MDA8}$ during high-ozone episodes of October 2010. Purple and blue lines represent + 1 K and + 2 K temperature perturbations in the boundary layer, respectively. Solid lines show only the impact of temperature on chemistry and dashed lines show the temperature impacts on both chemistry and biogenic emissions.

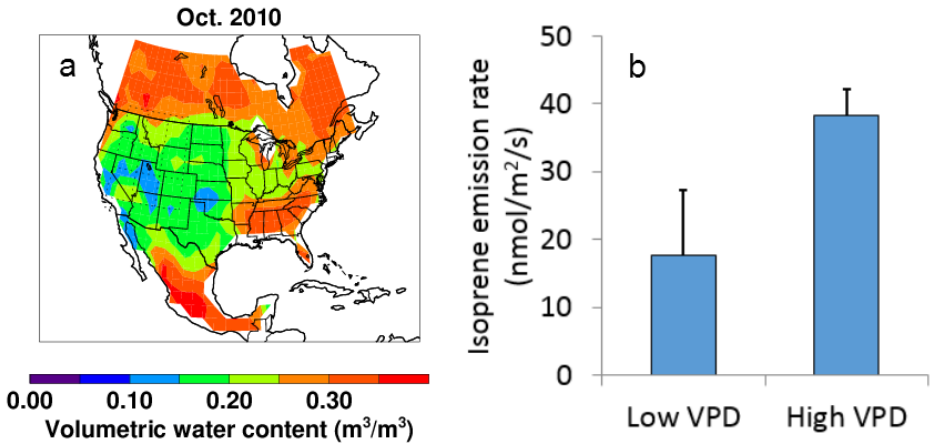

Figure S11. Enhanced isoprene emissions when VPD is high but soil moisture is not a limiting factor. a, Monthly mean volumetric soil moisture from 20 cm to 200 cm below the surface in October 2010 from the NCEP-DOE reanalysis. Soil moisture in most areas of the SE is > 0.3 m^3/m^3, well above the reported wilting point (ranging from 0.04-0.23m^3/m^3) (5, 6). **b,** The experiment conducted in Biosphere 2 shows that the isoprene emission rate is enhanced by a factor of two from low VPD (humid) condition (~1 kPa) to high VPD (dry) condition (~3 kPa). **b** is adopted from data published in Pegoraro et al. (7).

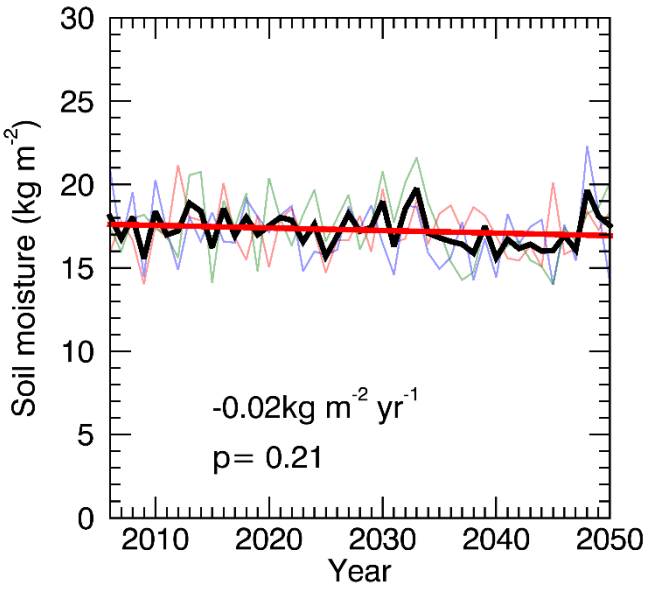

Figure S12. The mean projection from the GFDL model ensemble (3 ensemble members, RCP 4.5) shows an insignificant trend of top soil (< 10 cm) moisture (-0.02 kg m^{-2} yr^{-1}, p=0.21) over the SE in October from 2006 to 2050. Thin colored lines are ensemble members. Thick black and red lines represent the ensemble mean and linear trend, respectively.

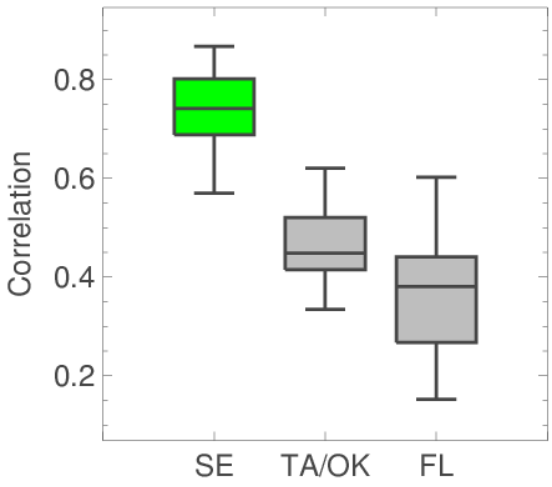

Figure S13. Correlation between $[O_3]_{MDA8}$ at individual sites with the SE regional average during October from 1980 to 2010. The box and whisker plots show median (black line inside boxes), lower and upper quartiles (boxes), and 5th and 95th percentiles (whiskers). The SE region is defined in Fig. 1. Ozone at the sites within the SE region are well correlated with the SE regional average (green box), showing that the regional average is representative. Ozone at the sites in Texas/Oklahoma and Florida are not well correlated with the SE regional mean (gray boxes), reflecting that weather systems influencing these regions are often different from those influencing the main SE region.

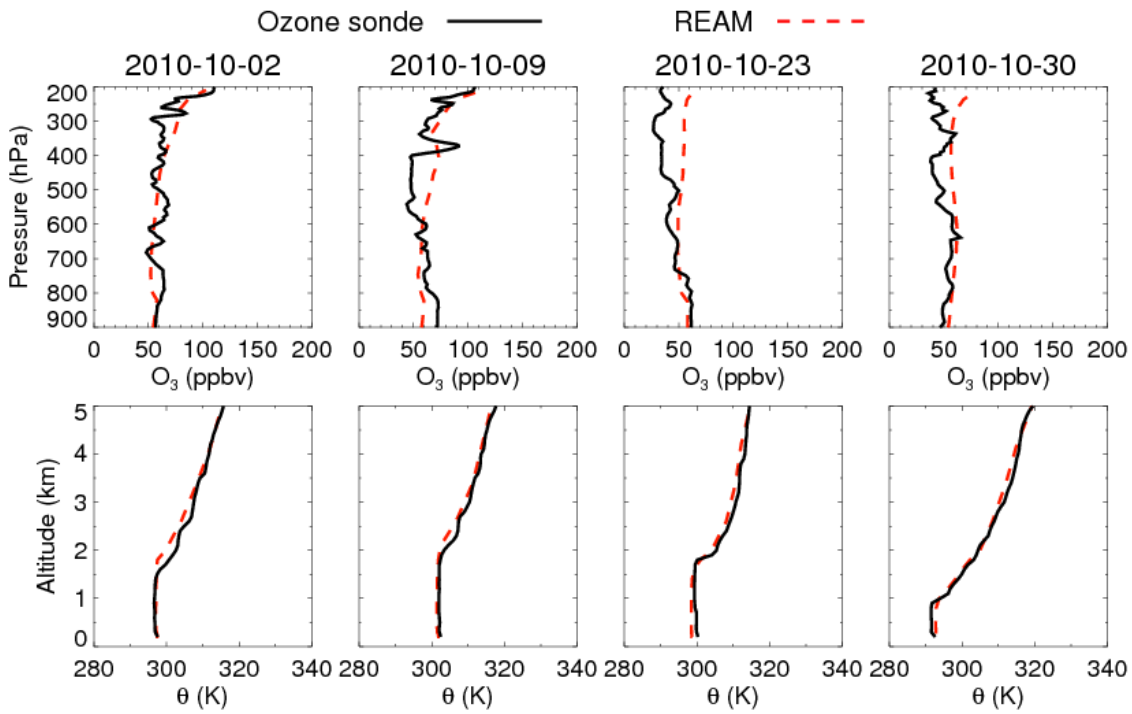

Figure S14. Comparison of ozone and potential temperature (θ) between model simulations and ozonesonde observations in Huntsville, Alabama on 2nd, 9th, 23rd, and 30th of October, 2010.

200

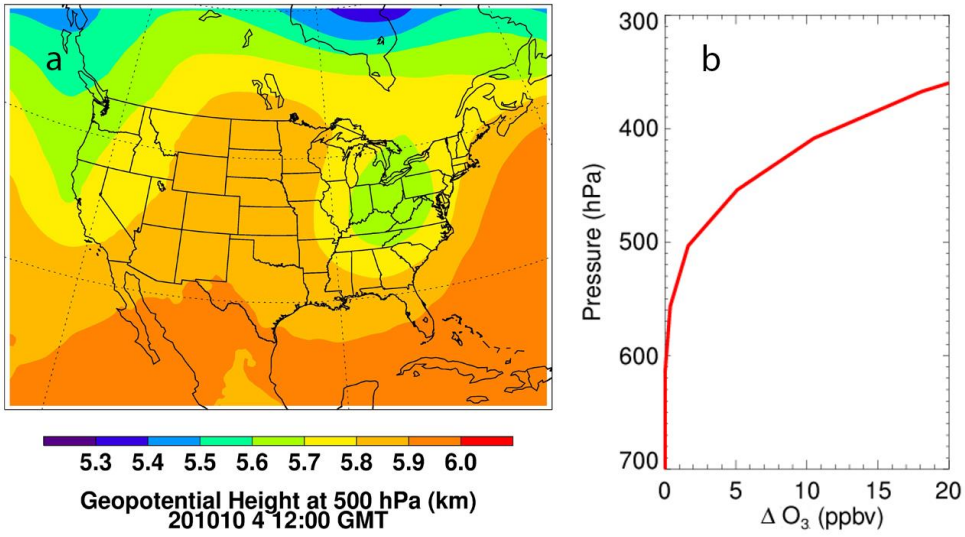

Figure S15. a, The cut-off low system over the eastern U.S. favoring stratospheric intrusion on Oct. 4, 2010. Data is computed using the WRF-assimilated meteorological field inputs to the REAM. **b**, The REAM-calculated vertical profile of ozone enhancement resulting from stratospheric intrusion over the SE on Oct 4, 2010.